Ecological Indicators 159 (2024) 111624

Contents lists available at ScienceDirect

Ecological Indicators

journal homepage: www.elsevier.com/locate/ecolind

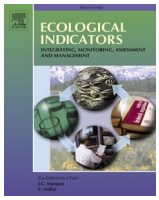

Original Articles

Characterization of forest edge structure from airborne laser scanning data

Moritz Bruggisser [a,*], Zuyuan Wang [a], Christian Ginzler [a], Clare Webster [b,c], Lars T. Waser [a]

[a] Swiss Federal Institute for Forest, Snow and Landscape Research WSL, Zürcherstrasse 111, 8903 Birmensdorf, Switzerland
[b] Department of Geosciences, University of Oslo, Oslo, Norway
[c] WSL Institute for Snow and Avalanche Research SLF, Flüelastrasse 11, 7260 Davos Dorf, Switzerland

ARTICLE INFO

Keywords:
Vegetation structure
National forest inventory
Shelterbelt
Light availability

ABSTRACT

Forest edges represent the transition zone (ecotone) between the forest interior and the surrounding open land. Due to their great ecological importance, the value of assessing the structure of forest edges has been recognized. In Switzerland, for example, forest edge structure is assessed during field surveys of the Swiss National Forest Inventory (NFI). However, these assessments are time consuming and limited to sample plots. Publicly available countrywide airborne laser scanning (ALS) data, in contrast, offers possibilities to retrieve forest edge structure information over large spatial extents. In this study, we derived five metrics from ALS point clouds, namely the canopy height variability; ratios of the areas of the three edge components, i.e. shrub belt, shelterbelt and forest layer; the sky-view fraction; the shelterbelt slope; and the front density of the forest edge. These metrics describe the three-dimensional edge structure and therefore could enhance existing NFI edge metrics, which focus on two-dimensional structure characteristics. An expert assessment of the ALS edge metrics demonstrated the ability of the defined set of edge metrics to capture ecologically relevant and indicative characteristics of forest edges. Understanding this relationship between edge metrics and ecological functions is a prerequisite if ALS metrics are to be integrated into NFIs. We subsequently used the ALS edge metrics to group 284 forest edge into three classes with respect to their structural complexity using k-means clustering. The results indicated that the structual complexity was low for 173, medium for 46 and high for 65 forest edges, respectively. Applied to countrywide ALS data sets, our approach allows to retrieve area-wide, spatially continuous information on the forest edge conditions, and, if multitemporal ALS data is available, to monitor the development of the forest edges.

1. Introduction

Forest edges are the transition zones, i.e. ecotones, between the forest interior and the surrounding ecosystems, such as grasslands, wetlands and agricultural areas. As such, they are important for the ecosystem functioning (Harper et al., 2005; Wang et al., 2020; Meeussen et al., 2021) including maintenance of biodiversity (de Casenave et al., 1995; Verhelst et al., 2023). The structure of the forest edge, i.e. the three-dimensional (3D) arrangement of biomass, emerges as a key factor determining its ecosystem functioning (Harper et al., 2005; Meeussen et al., 2021). A natural forest edge consists of a shrub belt and a shelterbelt, with a distinct height gradient from the open land to the forest interior (cf. Brändli, 2001, p. 275, Fig. 2). Furthermore, ideal forest edges are characterized by an increased light availability compared with the inner forest (de Casenave et al., 1995; Verhelst et al., 2023).

Consequently, the structural composition of forest edges impacts the magnitude and extent of the ecosystem services that these ecotones are able to provide (Harper et al., 2005). Human impacts, however, have led to more abrupt forest edges, often lacking a gradual transition in their structure, impairing the functioning of the forest edges (Harper et al., 2005; Wang et al., 2020).

Due to its importance for ecosystem functioning, edge structure is often assessed in forest inventories. So far, this has mainly been accomplished through field assessments, which are labor-intensive and therefore limited to sample plots. In Switzerland, for example, forest edges have been operationally and repeatedly assessed since the second iteration of the Swiss National Forest Inventory (NFI; cf. Brändli and Ulmer, 1999).

In comparison to such field work, remote sensing technologies can be used to acquire the necessary information over large areas at a relatively low cost (White et al., 2016). With airborne laser scanning (ALS), the 3D forest structure is acquired at a high level of detail and over large spatial extents. Therefore, ALS makes it possible to retrieve objective estimates of forest attributes and has been frequently used in forest inventories (White et al., 2013; Næsset, 2014; Maltamo et al., 2021) or for forest habitat characterization (e.g. Coops et al., 2016; Bourgouin et al., 2022;

* Corresponding author.

https://doi.org/10.1016/j.ecolind.2024.111624
Received 31 October 2023; Received in revised form 8 January 2024; Accepted 17 January 2024
Available online 28 January 2024

Huo et al., 2023). Few studies, however, have involved using ALS data to retrieve information on forest edge structure and conditions, although the great value this data offers for the task of forest edge characterizations has been illustrated in Wehrli (2015),Bühler and Zurschmiede (2017) and Wang et al. (2020). The great potential of ALS additionally results from the repeated and publicly available data with high point densities, that is now provided by many national and local authorities.

The goal of our current work was to comprehensively harness the 3D information provided by ALS data. We expanded the structure descriptions by Wehrli (2015) and Wang et al. (2020), who focused on two-dimensional (2D) edge characteristics, and we aimed to describe the 3D composition of the forest edges in more detail, particularly the structure of the shelterbelt. We utilised five metrics (canopy height variability, area ratio of edge components, sky-view fraction, shelterbelt slope, and front density) that are indicative of forest edge structure and have ecological significance, meaning that they are comprehensible and easy to interpret. The application of the forest edge description is first demonstrated for individual sample points comprising forest edges which include a wide range of forest edge types. Second, we illustrate how the approach can be applied on landscape scale to describe the forest edge structure in a spatially continuous way. Ultimately, the spatially explicit 3D edge characteristics we derive from ALS data provide a complementary information layer to the existing field-based forest edge assessments. Likewise, forest edge information on the scale of entire landscapes can be retrieved where such data from field-based assessments is missing.

2. Materials and methods

2.1. Study area

Switzerland is located in Central Europe (45–48° N, 5–11° E). The topography is heterogeneous, with flat landscapes in the Central Plateau and steep slopes in the Alps, and elevations range from 193 to 4634 m a.s.l (Fig. 1). A third of the country is covered with forests (approx. 1.32 Mio ha.), of which 42% are pure coniferous and 24% are pure deciduous stands. Of the total forest area, 17% is located in the Central Plateau and 18% in the Prealps, while 35% lies in the Alps. The total forest edge length for the entire country amounts to 115,000 km. The main forest functions in Switzerland are protection against natural hazards (46%) and timber production (31%). More details on the forest distribution and development in Switzerland can be found in Brändli et al. (2020).

A 6,500 m x 1,050 m (east–west by north–south extent) test site was subset to demonstrate the forest edge characterization over an area-wide extent. The test site is located in the north of Switzerland (star in Fig. 1) and covers the northern slope of Lägern ridge with elevations up to 820 m above sea level. The area is characterized by mixed forest dominated by European Beech (*Fagus sylvatica* L.), and mainly surrounded by agricultural area. The total length of the forest boundary line within the subset measured 9,200 m. The selected area is representative for landscapes in the Central Plateau and the Prealps. These areas are characterized by agriculture and a conflict of interest with sustainable forest management with ecologically valuable forest edges. Therefore, we see the greatest benefit of our forest edge description for such areas, while mountainous forest and particularly forest edges at the upper timber line were not in focus.

2.2. Data

2.2.1. Laser scanning data

The forest edge description metrics are based on the swissSURFACE3D ALS point cloud data set (cf. swisstopo, 2022b). The data set is acquired and provided by the Swiss Federal Office of Topography (swisstopo) and is openly accessible. The latest version of the data set was acquired during the leaf-off season between 2017 and 2023. Nominal point densities range from 15 to 20 pts/m^2 with a minimum of 5 pts/m^2, while the point densities are higher in forested areas, with a mean of around 30 pts/m^2.

2.2.2. Sample points from field visits

We used sample locations of the NFI to validate our approach, if a respective NFI plot comprised a forest edge (approx. 500 of the 6,600 NFI plots; Düggelin et al., 2020). Since the NFI plots are considered to be representative for the countrywide forest conditions, we expected that they comprise a wide variety of possible forest edge compositions. We used intermediate results from the fifth inventory phase of the NFI (NFI 5, 2018–2026), which cover the years 2018–2022 and which was conducted concurrently with the ALS acquisition campaign by swisstopo. Since point clouds from some parts of Switzerland were not available at the time of the study, however, we ultimately considered a total of 284

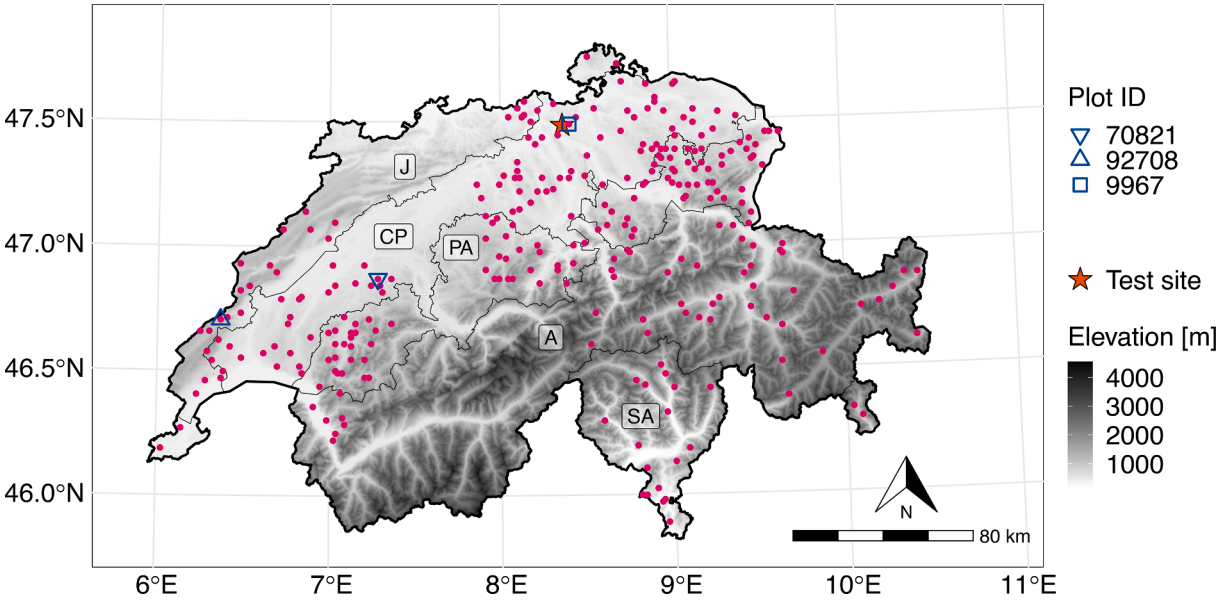

Fig. 1. Spatial distribution of the 284 Swiss NFI sample points that contain forest edges and for which swissSURFACE3D acquisitions were available. Marked are the locations of the example forest edge zones (Edge ID 9967), and Edge zones 70821 and 92708. The star indicates the location of area-wide forest edge description. Regions: J: Jura; CP: Central Plateau, PA: Prealps; A: Alps; SA: Southern Alps. Source: swisstopo.

NFI sample points containing forest edges (Fig. 1).

2.2.3. Auxiliary data

We used the forest boundary line from the NFI countrywide forest mask. This forest boundary line served as a reference line to place the sample points and to delineate the forest edge zones. The forest mask is based on a digital surface model (DSM) from digital aerial stereo-images with a spatial resolution of 1 m. Detailed information on the forest mask is given in Waser et al. (2015).

To normalize the point cloud before deriving the edge structure metrics, we interpolated a digital terrain model (DTM) from the point cloud. We used the point classification with which the ALS data was delivered and used ground points only for the calculation of the DTM.

2.3. Forest edge zone preparation

We calculated the edge metrics within the entity of an edge zone, centered at the sample point *s* (Fig. 2). The idea of characterizing forest edges on the basis of a fixed defined spatial extent originates from field-based forest edge description frameworks (e.g. Krüsi and Schütz, 1994). Following Wang et al. (2020), we defined the edge zone as a 100 m $\times$ 60 m area: the total edge zone length measures 100 m along the forest boundary line (50 m in both directions from the sample point *s*; cf. Fig. 2, light pink line, distances $\overline{se1}$ and $\overline{se2}$). The width of the edge zone is 60 m, centered at the sample point and measured perpendicular to the forest boundary line (Fig. 2, white line with $\overline{sp1}$ and $\overline{sp2}$ corresponding to distances of 30 m inside and outside of the forest, respectively).

Within the edge zone, we removed land cover elements that would have distorted the edge metrics, for example farmhouses. We only selected vegetation points from the point cloud, completely omitting points classified as buildings from the workflow. Furthermore, we excluded agricultural areas within the edge zones, using a land-use map compiled from cantonal land-use information. Finally, we excluded isolated trees or bushes in front of the forest edges. The criterion for their detection was a minimum distance of 6 m covered with no vegetation (vegetation height $<$ 0.5 m) between these objects and the cohesive forest edge.

2.4. Edge structure metrics

We calculated five metrics within the forest edge zone (Table 1). The metrics can be divided into zonal metrics and profile metrics, depending on the reference unit from which they were derived. We calculated zonal metrics based on the canopy height model (CHM) for the entire edge zone. We generated a CHM with a resolution of 0.5 m from the point cloud. In contrast, profile metrics were calculated along five discrete profiles arranged at equal intervals within the edge zone (distance between two profiles measures 20 m along the forest boundary line), with the middle profile crossing the sample point *s* (Fig. 3a). We considered the entire length of the profile when computing the profile metrics, i.e. the edge zone borders marked the end points of the profiles.

2.4.1. Height variability

The height variability describes the heterogeneity of the canopy heights within the edge zone. We calculated this metric from the CHM with 0.5 m spatial resolution as:

$$heightvariability = \frac{sd(CHM)}{mean(CHM)} \quad (1)$$

Table 1
Overview of the five derived edge metrics. The data source column lists the major products from which the respective metrics were derived (either from the canopy height model (CHM) or directly from the point cloud). The category column indicates whether the calculation was performed on the level of the entire forest edge zone (zonal metric) or based on individual profiles (profile metric).

Edge metrics	Data source	Category
Height variablity	CHM	Zonal metric
Edge components	CHM	
Sky-view fraction	CHM	
Shelterbelt slope	CHM	Profile metric
Front density	Point cloud	

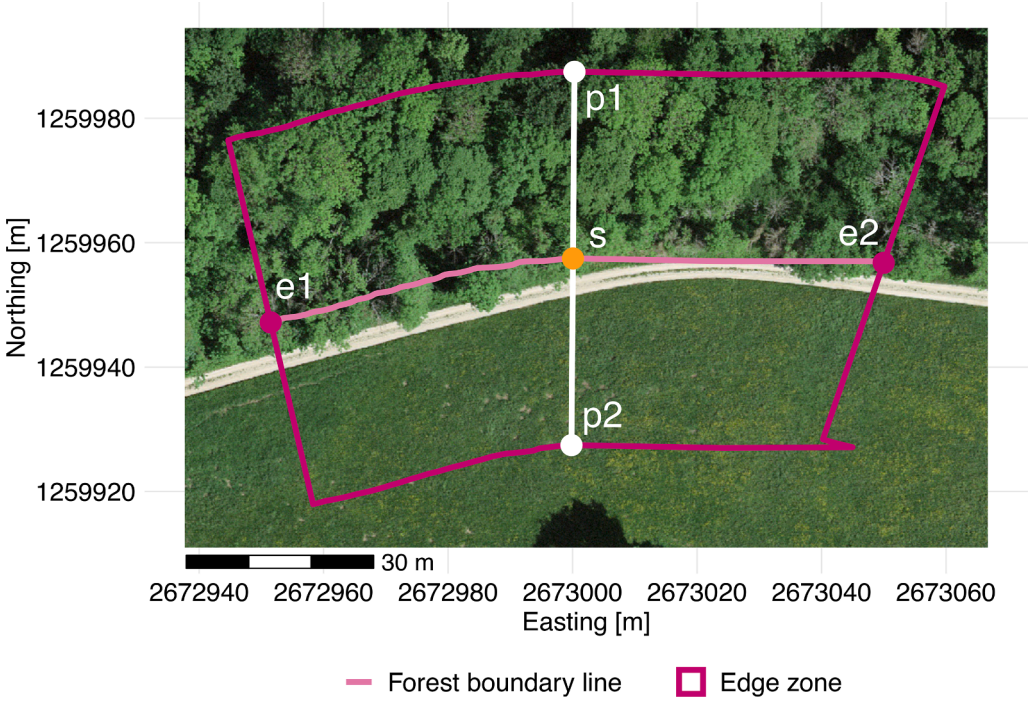

Fig. 2. Outline of the forest edge zone extracted around a sample point *s*. The white line is perpendicular to the forest boundary at *s* and corresponds to the width of the edge zone. Source: swisstopo.

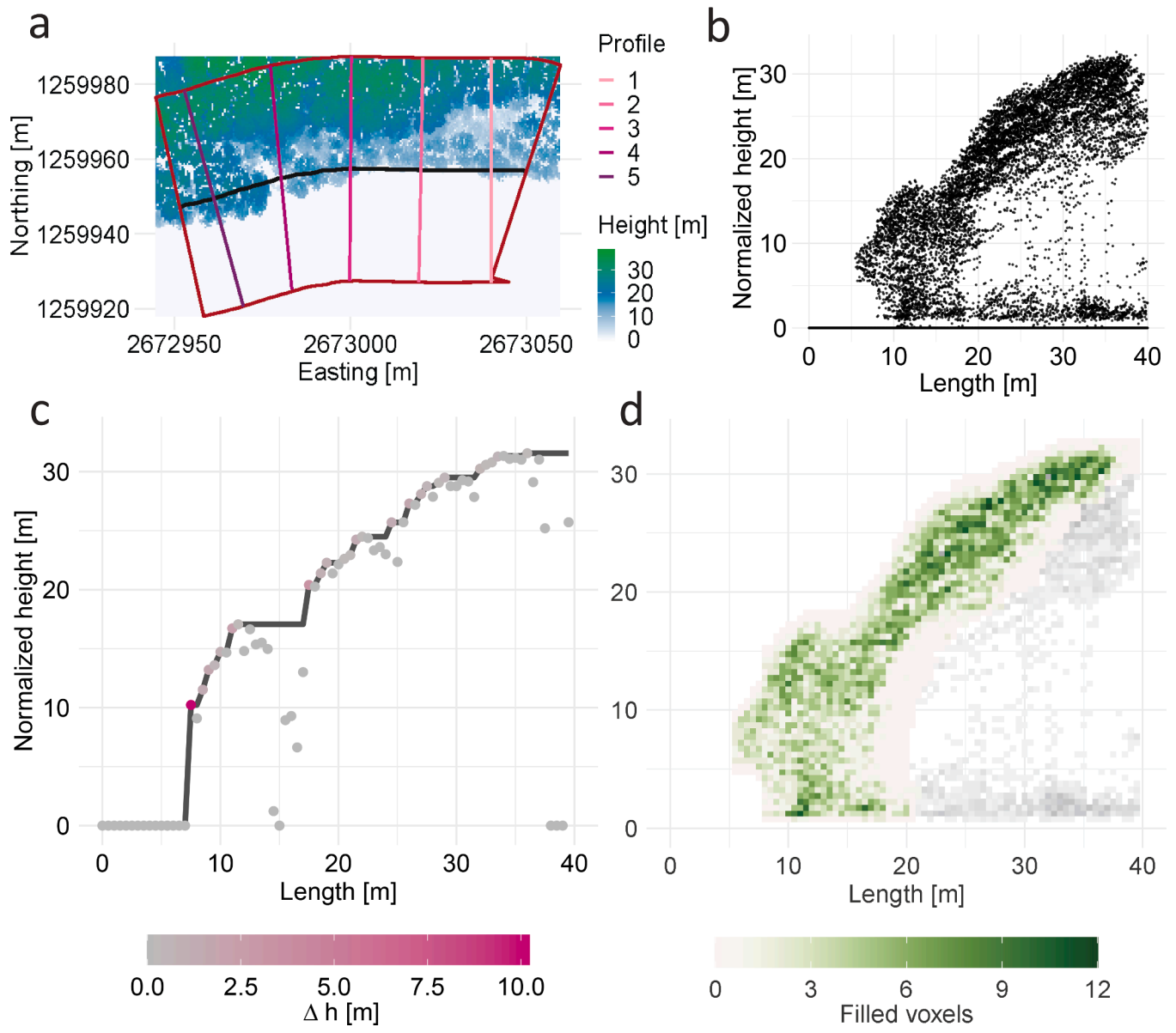

Fig. 3. (a) Overview of the edge zone, with the canopy height model (CHM) overlaid with the five profiles for which the profile metrics were computed. (b) Normalized point cloud transect (width = 10 m) taken along profile 3 (middle profile in (a)). (c) CHM profile along profile 3. Depicted are the original CHM values (dots) and the increasing height profile (solid line). The color of the dots refers to the height increase in the increasing height profile (basis for structure feature *max_dh*). (d) Side view of the voxelized point cloud in (b). The colors indicate the number of filled voxels in the forest front, aggregated in the direction across the profile width. Non-front voxels in the side view profile are grayed out.

where *sd* refers to the standard deviation of the CHM heights and *mean* to average CHM value within the edge zone.

2.4.2. Edge components

Considering the definitions in Krüsi and Schütz (1994), we separated the forest edge zone into three components, i.e. forest (canopy height $h \geqslant 16$ m), shelterbelt (4 m $\leqslant h < 16$ m) and shrub belt ($h < 4$ m), based on the height thresholds which were used in Wehrli (2015). We applied these height thresholds to the CHM to retrieve the areas of the respective edge components within the forest edge zone (cf. Wang et al., 2020). Finally, we calculated the ratio of each of the three components with respect to their total area. For the example of the shrub belt fraction:

$$fraction_{shrub} = \frac{A_{shrub}}{A_{shrub} + A_{shelterbelt} + A_{forest}} \quad (2)$$

2.4.3. Sky-view fraction

The sky-view fraction describes the visible portion of the sky in the hemisphere when a zenith-facing camera is placed on the ground, weighted by the cosine of the zenith angle (Webster et al., 2020) and characterizes the light availability at the forest floor. We calculated sky-view fraction from synthetic hemispheric images created using the approach by Webster et al. (2023, code available from https://github.com/c-webster/CanRad.jl), which calculates the light transmission through the canopy based on the CHM of the forest edge zone, terrain elevation data (for which we used the swissALTI3D data, cf. swisstopo, 2022a), and the forest mixture ratio between deciduous and conifer trees (cf. Waser et al., 2021). Images were created at 1.5 m height along a regular 2 m spaced grid across each edge zone.

We then summarized the sky-view fraction for each edge zone using two measures. First, we calculated the mean sky-view fraction within the entire forest edge zone (structure feature *skyview_plot*). Second, we

calculated the mean sky-view fraction for the forest part only of the forest edge zone (structure feature *skyview_forest*), where the separation between forest and non-forest was based on the forest mask. We considered this subdivision meaningful since the high sky-view fractions in the open land distort the average metric when included for the entire edge zone.

2.4.4. Shelterbelt slope

The shelterbelt slope describes nature of the transition between the open land and the forest interior. We characterized the shelterbelt slope using four measures: the maximum height increase and the distances to the 50%-, 75%- and 95%-height quantiles with respect to the maximum canopy height in the profile. Conceptually similar metrics were used in Verhelst et al. (2023). Heights were extracted from the CHM along each of the five profiles at the resolution of the CHM (0.5 m). For the processing, we reoriented the profiles – which were originally oriented perpendicular to the forest boundary line – such that the open land was on the left and the forest interior was on the right (Fig. 3b). This reorientation was necessary to obtain consistent measures for all profiles. To measure the maximum height increase, we transformed the profile into an increasing height profile (Fig. 3c, black line), where we only considered increases with respect to the previously achieved heights from the surrounding open area into the forest, neglecting decreases in the profile. The maximum height increase corresponds to the maximum increase in this increasing height profile. In contrast, we derived the distances to the three height levels from the actual CHM transects, where the reference ground point from which the distances were measured corresponded to the last canopy height value < 0.5 m before the canopy height increases.

2.4.5. Edge front density

The edge front density describes the openness of the forest edge front in the horizontal orientation. The computation of this metric was based on point cloud transects taken along the edge profiles (Fig. 3a), with a transect width of 10 m (Fig. 3b). In a first step, we voxelized the point cloud transects into voxels with an edge length of 0.5 m (Fig. 3d) and classified them as filled voxels if they contained at least one point. In a second step, we computed the fraction of filled voxels with respect to the total number of voxels within the first 10 m of the forest edge front, deriving the fraction separately for the shrub layer and the shelterbelt layer.

2.5. Edge structure classes

Forest edges in the NFI are classified into the three quality classes “low”, “average”, and “high” based on the field assessed edge structure metrics (cf. Brändli, 2001, p. 279, for more details on the retrieval of the edge quality classes). Following the NFI, we applied three target classes and applied k-means clustering (Hartigan and Wong, 1979), which is an unsupervised classification method. In contrast to the NFI, the unsupervised classification approach therefore clusters the edges in groups with similar structural characteristics instead of providing a classification of their ecological value.

We described each of the 284 forest edge zones using 12 structure features, which we derived from the five edge metrics (Table 2). The transformation of the edge metrics into structure features was necessary since we wanted to summarize the information of the respective metrics in one value per feature and edge zone. We applied this step to the sky-view fraction, which we had calculated within a 2 m raster in the first step and which we aggregated to a single value on the level of the edge zone, and to the profile metrics (*shelterbelt slope*, *front density*), which we summarized as the mean value of the five profiles per edge zone.

We individually normalized all structure features to the range [0, 1] before using them in the clustering.

3. Results

3.1. Edge structure metrics

Figs. 4 and 5 illustrate how the forest edge structure is captured for two exemplary edge zones from the NFI sample points. Figs. 4c and 5c show the edge components (shrub belt, shelterbelt, forest layer) that were derived from the CHM. Figs. 4e and 5e illustrate the sky-view fraction. The fraction ranges from 0 (sky is invisible from a spot) to 1 (complete hemisphere is visible). The figures in the right column show the point cloud transect (Figs. 4b, 5b; profile width $= 10$ m), the CHM profile with the distances to the 50%-, 75%- and 95%-height quantiles (Figs. 4d, 5d), and the side view of the voxelized point cloud reporting the number of filled voxels in the forest front (Figs. 4f, 5f). For both edge zones, the profiles through the zone centers (profile 3) are shown.

For comparison, orthoimages of the two edge zones are shown in Fig. 6a (Edge zone 70821) and 6b (Edge zone 92708).

Edge zone 70821 in Fig. 4 represents a forest edge with little height variability (*cov_plot* $= 0.6$). The edge structure is dominated by forest (*frac_forest* $= 0.97$), whereas a shrub belt is completely absent (*frac_shelterbelt* $= 0.03$). The sky-view fraction suggests low light availability within the forest part considering the forest mask (*sky_view_forest* $= 0.1$). The transition from the open land into the forest features a distinct border with a steep slope (*max_dh* $= 24.9$ m, *rise_distance_h50* $= 0.5$ m). The forest front is rather open in both the shrub belt height layer (*front_density_shrub* $= 0.04$) and the shelterbelt layer (*front_density_shelterbelt* $= 0.05$) (a front view of the edge front is given in Fig. 7a).

In contrast, the forest edge zone 92708 in Fig. 5 is more diverse in its canopy height (*cov_plot* $= 1.1$) and comprises a distinct shelterbelt (*frac_shelterbelt* $= 0.46$) and a shrub belt (*frac_forest* $= 0.1$). Light availability within the forest is higher (*sky_view_forest* $= 0.19$) with a diverse illumination pattern (Fig. 5e). The CHM profile illustrates a gradual, slow height increase from the open land into the forest (Fig. 5d, *rise_distance_h50* $= 15.8$ m), with less abrupt height steps (*max_dh* $= 13.1$ m). The forest front is rather dense, both in the shrub belt height layer (*front_density_shrub* $= 0.18$) and in the shelterbelt layer (*front_density_shelterbelt* $= 0.13$). A front view of the edge front is given in Fig. 7b.

3.2. Area-wide application

Fig. 8 illustrates how forest edge characteristics along the forest boundary line can be derived in a spatially continuous way at landscape scale. The sample locations, at which the forest edge characteristics were derived, were placed along the forest boundary line such that the forest edge zones were immediately adjacent to each other (white outlines in Fig. 8b–e). Fig. 8b, c depict the classified forest edge components which

Table 2
Five edge metrics with the derived structure features.

Edge metric	Structure feature	Description
Height variability	*cov_plot*	
Edge components	*frac_shrub frac_shelterbelt frac_forest*	Fractions of the three edge components (Eq. 2).
Sky-view fraction	*skyview_plot skyview_forest*	Mean values within entire edge zone and within forest, considering the forest mask.
Shelterbelt slope	*max_dh rise_distance_h50 rise_distance_h75 rise_distance_h95*	Mean of the five profiles per edge zone.
Edge front density	*front_density_shrub front_density_shelterbelt*	Density within 0.5–4 m (shrub belt) and within 4–16 m (shelterbelt) above ground.

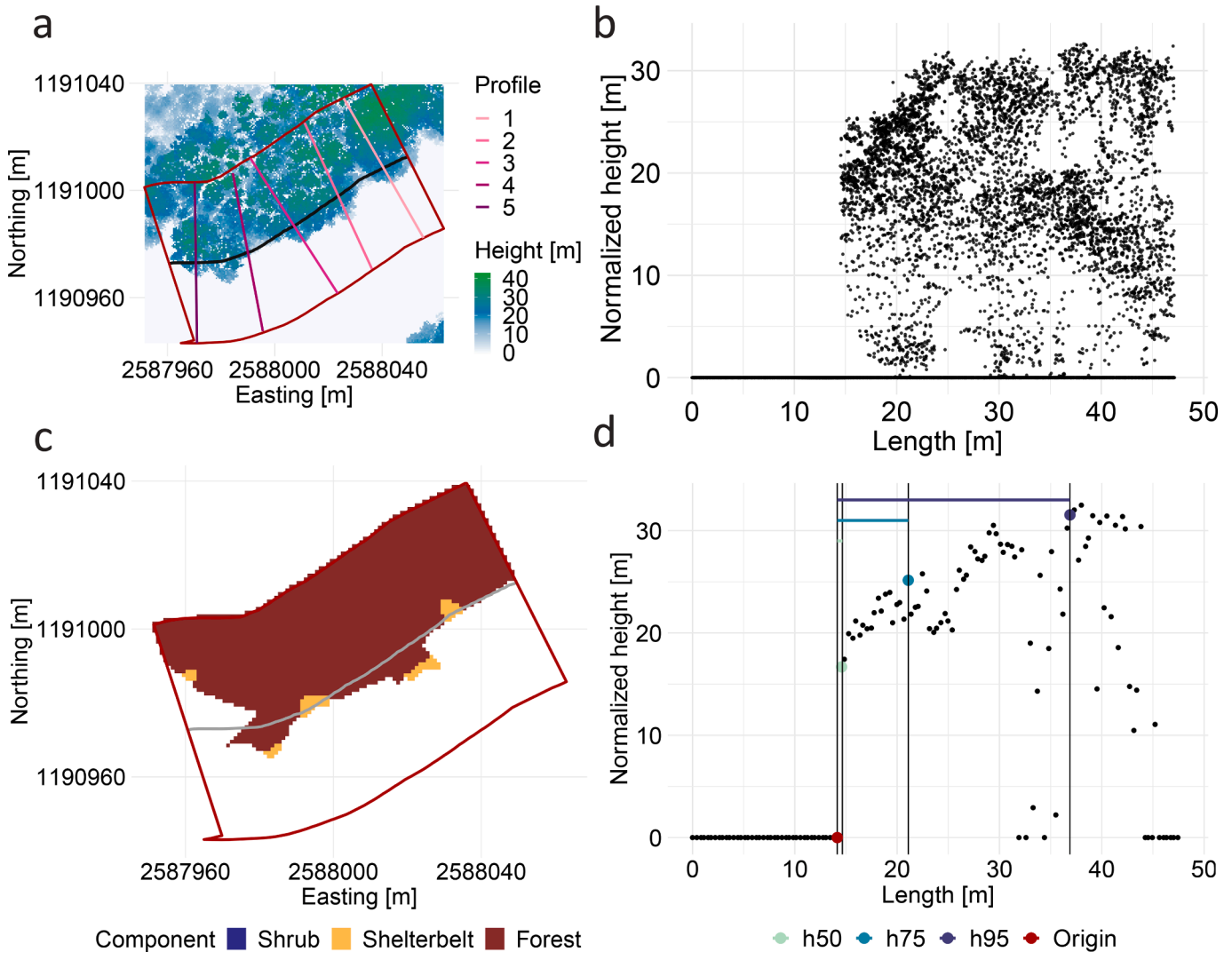

Fig. 4. Forest edge zone 70821. (a) Canopy height model (CHM) with the five profiles for which the profile metrics were calculated. (b) Point cloud transect from profile 3 (width = 10 m). (c) Classified edge components present within the forest edge zone. (d) Canopy height profile (black dots) from profile 3. Depicted are the distances to the 50%-, 75%- and 95%-height quantiles. (e) Sky-view fraction (value range [0, 1]) calculated in a 2 m raster. The white line marks the forest boundary line. (e) Side view of the voxelized and classified (filled/non-filled) point cloud transect from profile 3. The colors indicate the number of filled voxels in the forest front, aggregated in the direction across the profile width. Non-front voxels are grayed out.

form the basis for the calculation of the ratios of the shrub belt (*frac_shrub*), shelterbelt (*frac_shelterbelt*) and forest (*frac_forest*) within the forest edge zones. Fig. 8d, e show the maximum height increase (*max_dh*) along five profiles per edge zone. For clarification, the maximum height increase of individual profiles is shown but the values finally were aggregated to one value per edge zone.

For the two subsets, the fraction of shrub belt (*frac_shrub*), shelterbelt (*frac_shelterbelt*) and forest (*frac_forest*) ranged between 0.04–0.53, 0.23–0.39 and 0.23–0.66, respectively, for the five edge zones in ROI 1 and between 0.00–0.09, 0.05–0.23 and 0.69–0.93, respectively, for the five edge zones in ROI 2. Maximum height increases (*max_dh*), aggregated per edge zone, ranged between 12.8–18.2 m in ROI 1 and between 13.1–18.5 m in ROI 2.

3.3. Edge structure classes

K-means clustering of the 284 edge zones at the NFI sample points into three structure classes resulted in classes with 173, 46, and 65 edges. Table 3 summarizes the edge structure characteristics as the mean, median and standard deviation of the 12 structure features within the three classes. Actual distributions of the features within the three classes are shown in Fig. 9 (depicted is one structure feature per edge metric). Compared with Class 3, forest edges in Class 1 have a more homogeneous vegetation structure in terms of their height variability (mean *cov_plot* = 0.8 (Class 1) vs. 1.0 (Class 2) vs. 1.1 (Class 3)) and their edge structure consists mainly of the forest layer (*frac_forest* = 0.79 vs. 0.52 vs. 0.31). In particular, the shelterbelt in Class 1 is not very pronounced (mean *frac_shelterbelt* = 0.18 vs. 0.39 vs. 0.61), while the shrub belt is narrow or absent (mean *frac_shrub* = 0.02 vs. 0.09 vs. 0.08). Furthermore, the light availability is lower in Class 1 (*skyview_plot* = 0.29 vs. 0.35 vs. 0.43; *skyview_forest* = 0.17 vs. 0.23 vs. 0.31). Accordingly, Class 2 comprises edges with a structural composition in between the two other quality classes.

The profile metrics indicate that the forest edges in Class 1 are steep, which is reflected in the maximum height increase from the open land into the forest (*max_dh* = 13.7 m vs. 8.4 m vs. 8.2 m) and in the distance from the open land to the point where half of the maximum height of the profile is reached (*rise_distance_h50* = 2.4 m vs. 8.4 m vs. 2.6 m). Accordingly, forest edges in Class 2 and Class 3 exhibit a shelterbelt with a more gradual height increase than in Class 1, where this gradual nature

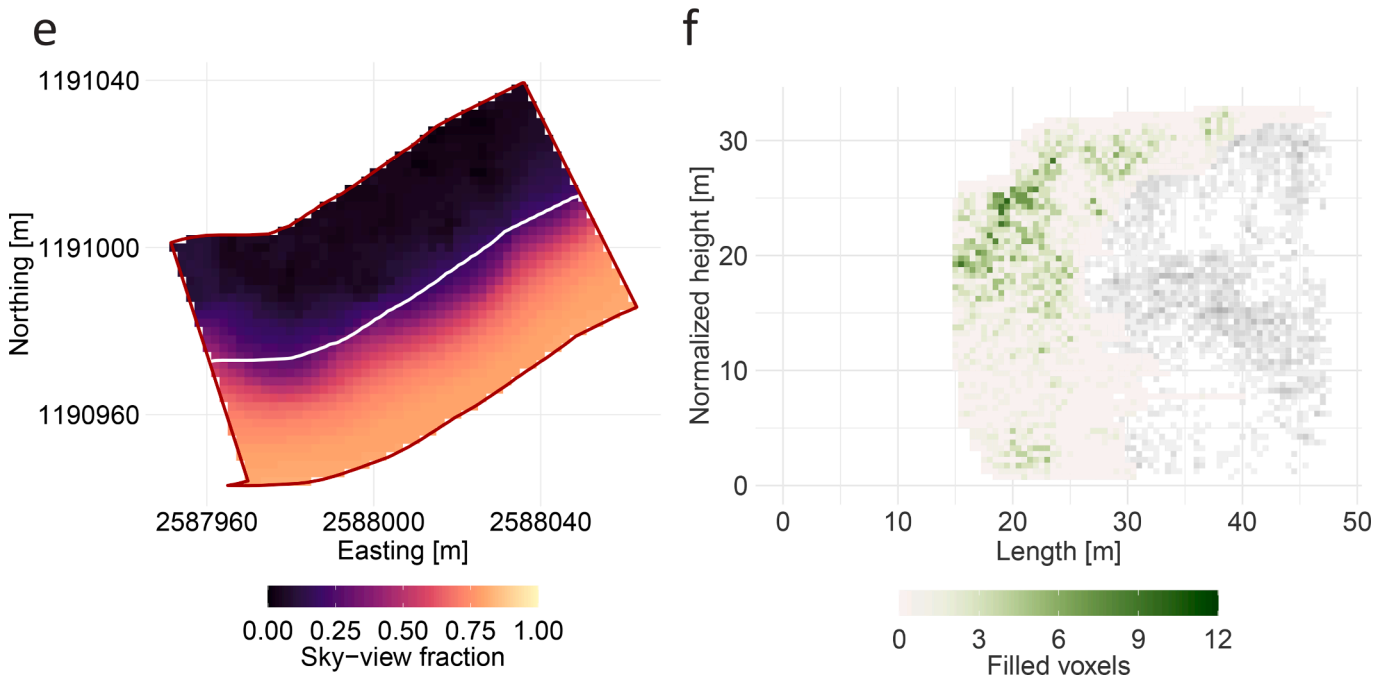

Fig. 4. (*continued*).

of the slope is most pronounced in Class 2. The density of the biomass in the forest edge front is lower in Class 1 than in the two other classes, both in the shrub belt height layer (0.5–4 m, *front_density_shrub* = 0.07 vs. 0.11 vs. 0.12) and in the shelterbelt height layer (4–16 m, *front_density_shelterbelt* = 0.09 vs. 0.13 vs. 0.12). Forest edges in Classes 2 and 3 therefore are more closed, with a reduced horizontal visibility into the forest from the front edge.

4. Discussion

4.1. Edge structure metrics

We defined five forest edge structure metrics that describe both the horizontal and the vertical composition of forest edges. The high point densities over forested areas enable detailed descriptions of the 3D structure, including the composition of the shelterbelt. We described the height composition of the edge by the height variability and the fractions of the edge components. While the height variability (*cov_plot*) summarizes the variability in canopy height on the level of the edge zone, the fractions of the three edge components (*frac_shrub*, *frac_shelterbelt* and *frac_forest*) describe the horizontal composition of the forest edges in more detail. The comparability of the height variability values is ensured since this metric is calculated from the CHM with a consistent spatial resolution of 0.5 m for all forest edges. The diverse topography in Switzerland results in forests with a high variability in tree heights. Therefore, we applied absolute height thresholds for the classification of the forest edge components to ensured that identical components are compared across a range of forest types. Similar to Verhelst et al. (2023), who described the forest edge structure from terrestrial laser scanning (TLS) data, we measured the height gradient of the shelterbelt with the four structure features *max_dh*, *rise_distance_h50*, *rise_distance_h75* and *rise_distance_h95*. The relevance of forest edges for various ecosystem services, inter alia, results from the higher light availability compared with in the forest interior (Ries and Sisk, 2004; Harper et al., 2005). We modeled the sky-view fraction to estimate the light regime. Finally, a dense edge front is important for shielding and protection of the forest interior from pollutant discharge from the surrounding open land (Wuyts et al., 2009). We introduced the front density metric to describe this structural characteristic of the forest edge. With this set of structure metrics, we provide a forest edge characterization which encompasses various aspects of forest edge structure properties. The metrics have a significance for the ecological functioning of the forest edge, are comprehensible and can be visually interpreted.

The validation of our metrics relied on expert assessments using maps and profile views of the forest edges, as depicted in Figs. 4 and 5. The figures showed examples of two forest edges, which differ greatly from each other. We observed that Edge zone 92708, compared to Edge zone 70821, was characterized by a more diverse height structure (*cov_plot*) and showed a more gradually increasing shelterbelt which is reflected in the maximum height increase (*max_dh*) and the distance from the front to half of the maximum canopy height (*rise_distance_h50*). Furthermore, the light regime within the forest area (*skyview_forest*) in Edge zone 92708 was more heterogeneous. The front density in the shrub belt height layer (< 4 m; *front_density_shrub*), was distinctly greater in the profile from Edge zone 92708. This was also visible in the front view of the voxelized edge profiles (Fig. 7) which showed that the shrub belt and lower parts of the shelterbelt height layer of the profile from Edge zone 92708 were more densely filled with biomass. However, the metric might be impaired by occlusion effects caused by the forest structure in the upper canopy parts, which result in a locally insufficient sampling with laser pulses given the applied flight acquisition scheme. The problem of insufficient representation of the forest edge front from ALS data should be investigated further in the future. Verhelst et al. (2023) also measured the density of the edge front, but using TLS. Since TLS data comprises a much higher level of detail and more information within lower vegetation layers than ALS data, TLS could serve as reference to evaluate the robustness of the front density towards ALS acquisition characteristics. We assume, however, that the high point density over forested areas, together with the generalization of the raw point cloud into classified voxels (filled/non-filled), reduces the impact occlusions have on the estimated density.

4.2. Area-wide edge structure retrieval from ALS data

ALS data makes it possible to derive spatially explicit information on the forest edge structure in a reproducible way. As demonstrated, forest edge information can be derived in a spatially continuous manner on an area-wide basis (Fig. 8). For this purpose, the sample points along the

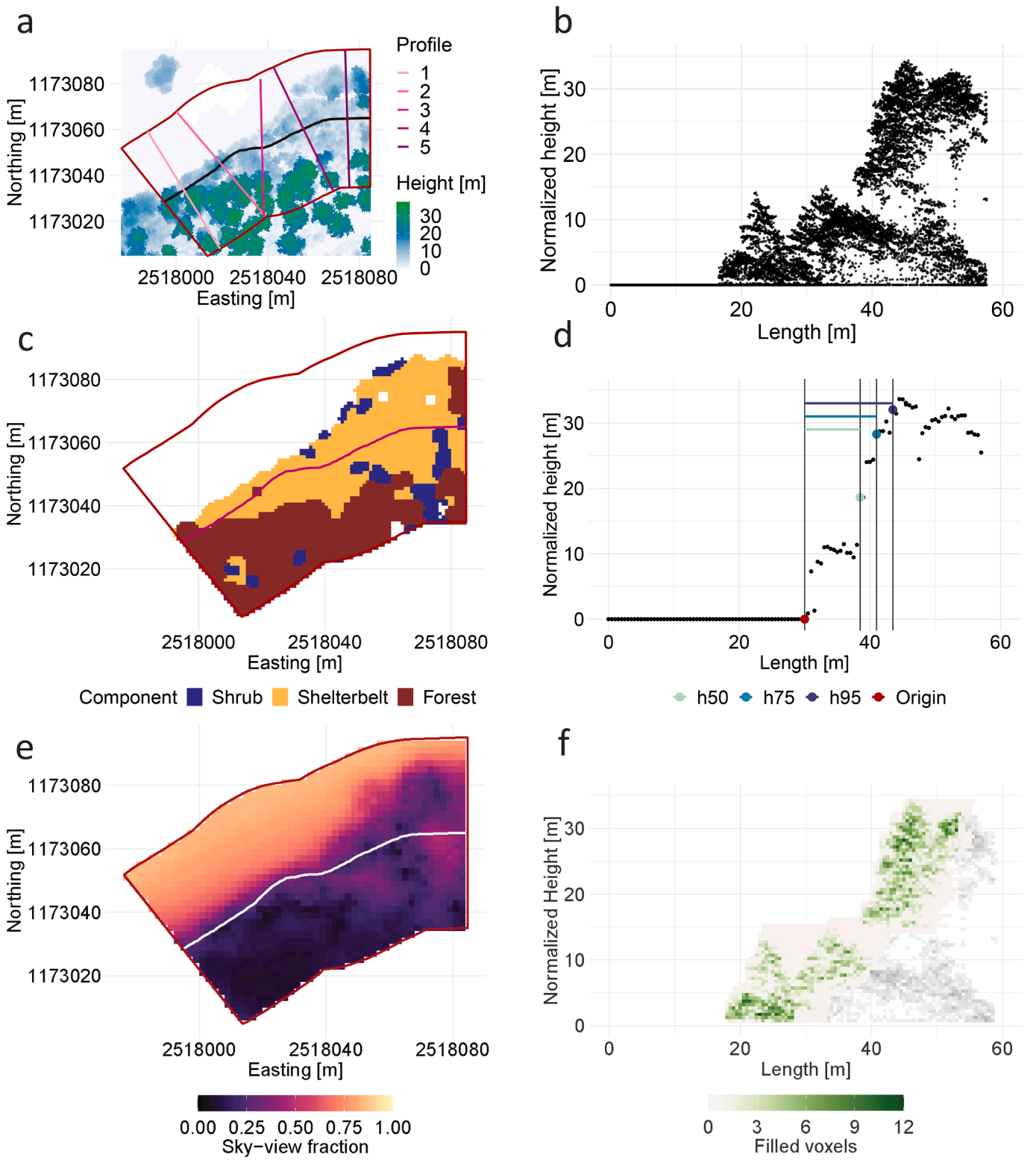

Fig. 5. Forest edge zone 92708. Cf. Fig. 4 for a detailed description. of the figures.

forest boundary line, which define the forest edge zones, were placed such that the forest edge zones were continuously adjacent to each other. Area-wide and spatially continuous forest edge information could be used to identify forest edges with certain structural properties, e.g. with low structural variability and steep slopes. An example of a forest edge section with low structural variability was visible in ROI 2 in the test site (Fig. 8c, e) where the forest edge mainly consisted of the forest component, whereas the shrub belt and shelterbelt were mainly missing. In contrast, the forest edge in ROI 1 (Fig. 8b, d) was structurally more diverse with a distinct shrub belt and shelterbelt. Spatially continuous edge structure information allows planning management activities such as forest edge restorations to increase their ecological value. In this context, multitemporal ALS data could enable the monitoring of forest edge development and efficacy of edge restoration activities, similar to

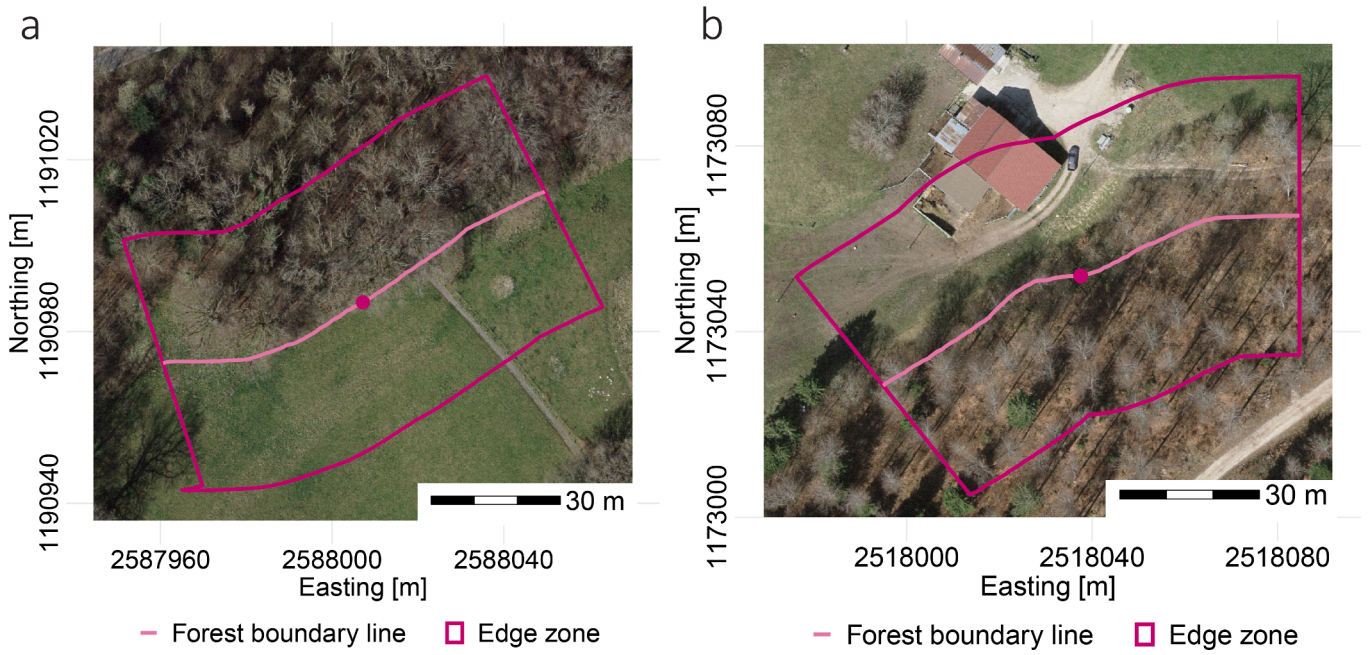

Fig. 6. Orthoimages for Edge zone 70821 (a) and for Edge zone 92708 (b), superimposed with the forest boundary line and the borders of the edge zone. The dark pink dot marks the edge zone center. Orthoimages were acquired in 2022. Source: swisstopo.

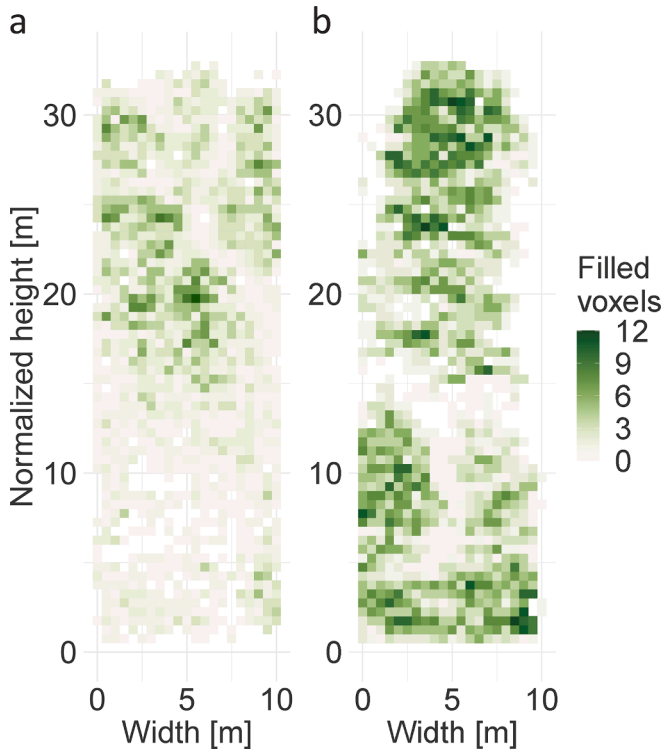

Fig. 7. Front view of the voxelized and classified (filled/non-filled) point cloud transects of profile 3 for Edge zone 70821 (a) and Edge zone 92708 (b). The voxel size is 0.5 m in all directions. The colors represent the number of filled voxels within the front 10 m of the forest edge, aggregated along the profile length.

Wang et al. (2020).

Furthermore, the derived edge characterization from ALS could be integrated into the NFI. Currently, the field-based forest edge descriptions in the NFI mainly include assessments of 2D structure characteristics and tree species information. The spatially explicit, 3D forest edge measurements from ALS point clouds therefore could be a valuable complement to the current NFI edge metrics.

4.3. Edge structure classes

We applied an unsupervised classification scheme to forest edges at NFI sample points to identify three edge classes with distinctly different structural characteristics. We observed that, compared with Class 3, forest edges in Class 1 had less height variability, a smaller or absent shrub belt, lower light availability within the forest structure, a steep shelterbelt slope, and a rather open forest front (Fig. 9 and Table 3). Class 2 represents an intermediate class. Compared with Class 3, edges in Class 2 comprised a larger area fraction that was covered with vegetation in the forest height layer (*frac_forest*), with a reduced shelterbelt (*frac_shelterbelt*); however, the composition of the shelterbelt was more gradual in this class than in Classes 1 and 3. Considering the composition of a natural forest edge in Brändli (2001), a forest edge with a high ecological value is associated with a gradual height transition. Consequently, the more diverse edge structure and more pronounced height transition found in Class 1 would indicate that forest edges in this class feature a higher ecological value than the forest edges in the two other classes. However, a definite assignment of the ecological value to classes from an unsupervised classification remains challenging. A potential improvement to our edge classification approach incorporates the replacement of the unsupervised classification with a framework that includes expert knowledge. Approaches to establish such a framework have been discussed for biomedical tasks (Valizadegan et al., 2013; Shamyuktha et al., 2022). Experts could define thresholds for the edge structure metrics that characterize the ecological value of the forest edges. Such a procedure is facilitated by the comprehensibility of the derived edge structure features which allow linking them to ecological functions. Such a classification offers the advantage of providing a wall-to-wall assessment of the ecological value of the edge ecotones based on ALS data (Wang et al., 2020). Ultimately, such a classification scheme would further increase the value of an ALS-based forest edge product for forest edge restoration and monitoring edge conditions over time.

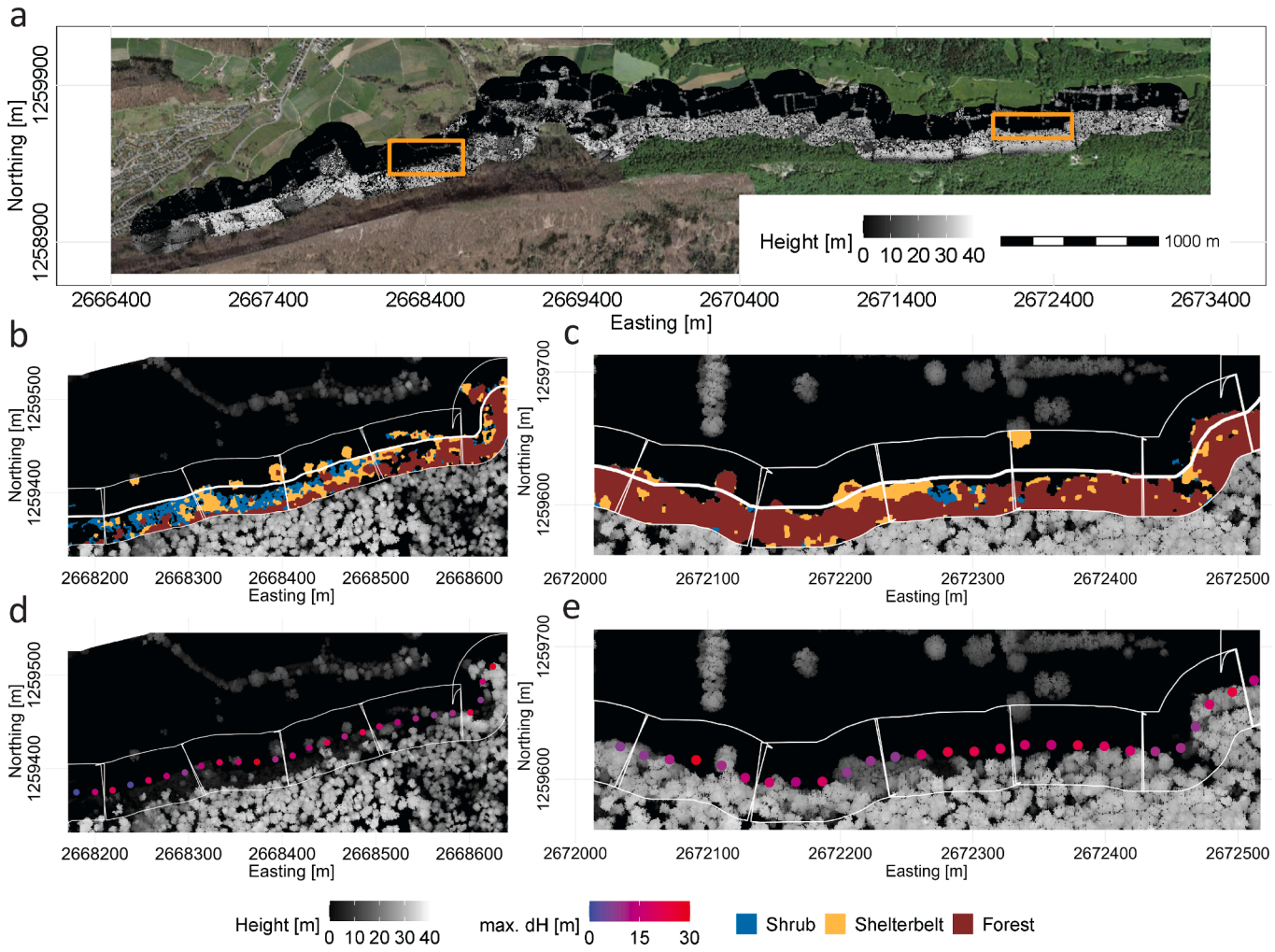

Fig. 8. Continuous edge description over a large extent illustrating how the forest edge zones are placed adjacent to each other in order to sample the forest edge in a continuous way. (a) Orthoimage of the entire area with the canopy height model (CHM) superimposed in the area of the forest edge (image source: swisstopo). The two rectangles (orange) mark the outlines of the two map insets in (b), (d) (ROI 1, rectangle to the west) and in (c), (e) (ROI 2, rectangle to the east), respectively. (b), (c) close-up maps showing the classified forest edge components (shrub belt, shelterbelt, forest) on top of the CHM. The thick white line represents the forest boundary. (d), (e) maximum height increase (*max_dh*) along the five CHM profiles per edge zone. The dots represent the positions of each of the profiles on the forest boundary (five per edge zone with a spacing of 20 m in between). The thin white lines in maps (b)–(e) represent the boarders of the forest edge zones for which the structure feature values are ultimately summarized.

Table 3
Summary of the 12 structure features describing the forest edges within the three edge quality classes. Reported are the mean, the median and the standard deviation (*sd*) for each structure feature and class. *max_dh*, *rise_distance_h50*, *rise_distance_h75* and *rise_distance_h95* are in [m] while all other features are unitless. The total number of edge zones in each of the three classes is also given.

	Class 1			Class 2			Class 3		
Structure feature	Mean	Median	sd	Mean	Median	sd	Mean	Median	sd
cov_plot	0.8	0.8	0.3	1.0	0.9	0.4	1.1	1.1	0.3
frac_shrub	0.02	0.01	0.03	0.09	0.05	0.10	0.08	0.05	0.10
frac_shelterbelt	0.18	0.17	0.11	0.39	0.39	0.14	0.61	0.60	0.18
frac_forest	0.79	0.81	0.12	0.52	0.52	0.15	0.31	0.34	0.18
skyview_plot	0.29	0.30	0.09	0.35	0.35	0.10	0.43	0.43	0.11
skyview_forest	0.17	0.16	0.06	0.23	0.20	0.10	0.31	0.28	0.12
max_dh	13.7	13.1	4.3	8.4	8.0	2.7	8.2	7.6	3.2
rise_distance_h50	2.4	2.0	1.6	8.4	8.6	4.6	2.6	2.6	1.6
rise_distance_h75	6.0	5.6	2.7	15.9	15.3	4.5	7.0	6.7	3.5
rise_distance_h95	14.3	14.7	4.8	22.8	22.7	5.3	13.4	13.7	5.9
front_density_shrub	0.07	0.06	0.03	0.11	0.10	0.05	0.12	0.11	0.06
front_density_shelterbelt	0.09	0.09	0.04	0.13	0.13	0.04	0.12	0.12	0.05
Total number of edge zones	173			46			65		

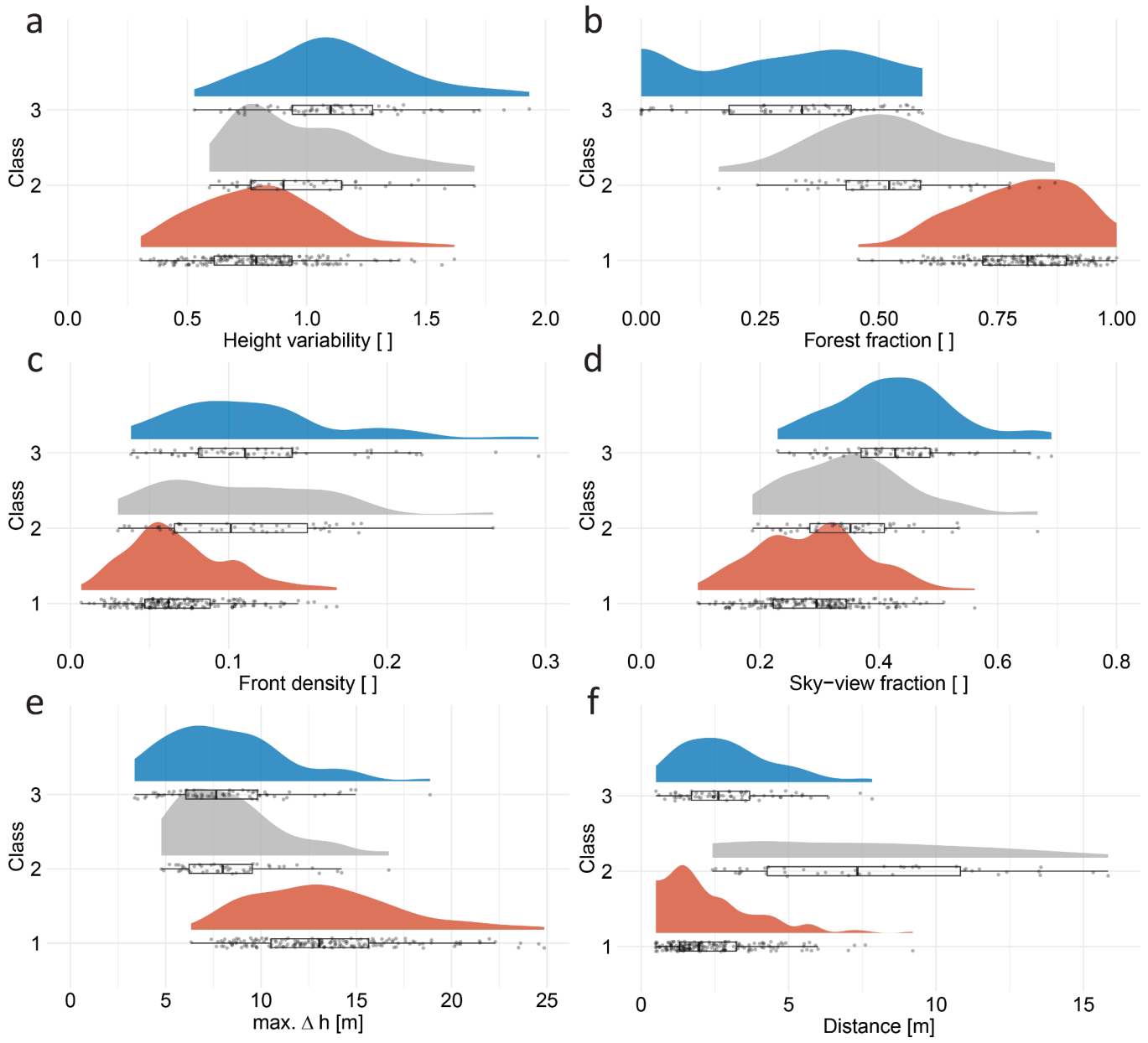

Fig. 9. Distribution of the structure features within the three edge quality classes. (a) Height variability (*cov_plot*). (b) Edge component fraction for forest area (*frac_forest*). (c) Front density within the shrub layer (*front_density_shrub*). (d) Mean sky-view fraction (*skyview_plot*). (e) Maximum height increase (*max_dh*). (f) Distance from the forest edge front to the 50%-height quantile (*rise_distance_h50*).

5. Conclusions

In the present study, we proposed five structure metrics (height variability, edge components, sky-view fraction, shelterbelt slope and edge front density) derived from ALS point clouds to characterize the 3D composition of forest edges. These metrics capture indicative characteristics of the edge structure, including detailed information on the shelterbelt, and at the same time have a clear ecological significance. The expert assessment of point cloud transects confirmed the metrics' ability to measure the intended structural properties.

ALS point clouds offer the advantage of providing spatially explicit edge descriptions that are both quantitative and qualitative. Moreover, the availability of countrywide ALS data enables to retrieve information on the structural conditions of forest edges over large areas in a spatially continuous way.

Area-wide information on the forest structure allows planning management activities to restore forest edges with decreased ecological value. Likewise, the proposed ALS metrics complement existing field-based forest edge assessments, which mainly focus on 2D characteristics of the forest edge composition. However, forest edge descriptions derived from ALS data cannot replace field assessments completely, especially as species composition, an important forest edge characteristic, cannot be derived from the point clouds in detail. We therefore believe that the greatest potential of our ALS edge metrics lies in the enhancement of existing NFI edge assessments.

The derived forest edge metrics further can be used to classify forest edges with regard to their structural properties. The link between the edge structure and the ecological value of the forest edge, however, is not straightforward. For a more indicative edge quality assessment based on ALS data, we propose to establish a classification scheme based on expert knowledge. This would increase the benefit of the classification because the quality classes would have a clearer ecological significance. Ultimately, such an improved forest edge quality map would enable the detection of degraded edges that require restoration, as well

as the monitoring of ongoing edge enhancement activities over large spatial extents.

Funding

This study was carried out in the framework of the Swiss National Forest Inventory (NFI), a cooperative effort between the Swiss Federal Institute for Forest, Snow and Landscape Research (WSL) and the Swiss Federal Office for the Environment (FOEN).

CRediT authorship contribution statement

Moritz Bruggisser: Conceptualization, Methodology, Software, Formal analysis, Visualization, Writing - original draft, Writing - review & editing. **Zuyuan Wang:** Methodology, Software, Writing - review & editing. **Christian Ginzler:** Conceptualization, Methodology, Writing - review & editing, Funding acquisition. **Clare Webster:** Software, Writing - review & editing. **Lars T. Waser:** Conceptualization, Methodology, Writing - review & editing.

Declaration of Competing Interest

The authors declare that they have no known competing financial interests or personal relationships that could have appeared to influence the work reported in this paper.

Data availability

Data will be made available on request.

Acknowledgments

We would like to thank Dr. Melissa Dawes for professional language editing.

References

Bourgouin, M., Valeria, O., Fenton, N.J., 2022. Predictive mapping of bryophyte diversity associated with mature forests using lidar-derived indices in a strongly managed landscape. Ecol. Ind. 136, 108585. https://doi.org/10.1016/j.ecolind.2022.108585.

Brändli, U.B., 2001. Nature protection function. In: Brassel, P., Lischke, H. (Eds.), Swiss National Forest Inventory: Methods and Models of the Second Assessment. WSL Swiss Federal Research Institute, Birmensdorf, Switzerland, pp. 265–282.

Brändli, U.B., Abegg, M., Allgaier Leuch, B. (Eds.), 2020. Schweizerisches Landesforstinventar. Ergebnisse der vierten Erhebung 2009–2017. Swiss Federal Institute for Forest, Snow and Landscape Research WSL, Birmensdorf. Federal Office of Environment, Berne, Switzerland.

Brändli, U.B., Ulmer, U., 1999. Naturschutz und Erholung, in: Brassel, P., Brändli, U.B. (Eds.), Schweizerisches Landesforstinventar. Ergebnisse der Zweitaufnahme 1993–1995. Swiss Federal Institute for Forest, Snow and Landscape Research WSL, Birmensdorf. Federal Office of Environment, Berne, Switzerland.

Bühler, C., Zurschmiede, G., 2017. Pflege von Waldrändern – Erfolgskontrolle mit Laserscanning (LIDAR). Zürcher Wald 2, 29–32.

de Casenave, J.L., Pelotto, J.P., Protomastro, J., 1995. Edge-interior differences in vegetation structure and composition in a Chaco semi-arid forest, Argentina. For. Ecol. Manage. 72, 61–69. https://doi.org/10.1016/0378-1127(94)03444-2.

Coops, N.C., Tompaski, P., Nijland, W., Rickbeil, G.J., Nielsen, S.E., Bater, C.W., Stadt, J. J., 2016. A forest structure habitat index based on airborne laser scanning data. Ecol. Ind. 67, 346–357. https://doi.org/10.1016/j.ecolind.2016.02.057.

Düggelin, C., Abegg, M., Bischof, S., Brändli, U.B., Cioldi, F., Fischer, C., Meile, R., 2020. Schweizerisches Landesforstinventar. Anleitung für die Feldaufnahmen der fünften Erhebung 2018–2026. Swiss Federal Institute for Forest. Snow and Landscape Research WSL, Birmensdorf, Switzerland.

Harper, K.A., Macdonald, S.E., Burton, P.J., Chen, J., Brosofske, K.D., Saunders, S.C., Euskirchen, E.S., Roberts, D., Jaiteh, M.S., Esseen, P.A., 2005. Edge influence on forest structure and composition in fragmented landscapes. Conserv. Biol. 19, 768–782. https://doi.org/10.1111/j.1523-1739.2005.00045.x.

Hartigan, J.A., Wong, M.A., 1979. Algorithm as 136: A k-means clustering algorithm. J. R. Stat. Soc. Ser. C (Appl. Stat.) 28, 100–108. https://doi.org/10.2307/2346830.

Huo, L., Strengbom, J., Lundmark, T., Westerfelt, P., Lindberg, E., 2023. Estimating the conservation value of boreal forests using airborne laser scanning. Ecol. Ind. 147, 109946. https://doi.org/10.1016/j.ecolind.2023.109946.

Krüsi, B.O., Schütz, M., 1994. Schlüssel zur ökologischen Bewertung von Waldrändern. Informationsblatt Landschaft 20, Swiss Federal Institute for Forest, Snow and Landscape Research WSL, Birmensdorf, Switzerland. Retrieved from: https://www.dora.lib4ri.ch/wsl/islandora/object/wsl:15031.

Maltamo, M., Packalen, P., Kangas, A., 2021. From comprehensive field inventories to remotely sensed wall-to-wall stand attribute data—a brief history of management inventories in the nordic countries. Can. J. For. Res. 51, 257–266. https://doi.org/10.1139/cjfr-2020-0322.

Meeussen, C., Govaert, S., Vanneste, T., Bollmann, K., Brunet, J., Calders, K., Cousins, S. A., De Pauw, K., Diekmann, M., Gasperini, C., Hedwall, P.O., Hylander, K., Iacopetti, G., Lenoir, J., Lindmo, S., Orczewska, A., Ponette, Q., Plue, J., Sanczuk, P., Selvi, F., Spicher, F., Verbeeck, H., Zellweger, F., Verheyen, K., Vangansbeke, P., De Frenne, P., 2021. Microclimatic edge-to-interior gradients of European deciduous forests. Agric. For. Meteorol. 311, 108699. https://doi.org/10.1016/j.agrformet.2021.108699.

Næsset, E., 2014. Area-Based Inventory in Norway – From Innovation to an Operational Reality, in: Maltamo, M., Næsset, E., Vauhkonen, J. (Eds.), Forestry Applications of Airborne Laser Scanning: Concepts and Case Studies. Managing Forest Ecosystems, 27. Springer, The Netherlands. 464pp, pp. 215–240.

Ries, L., Sisk, T.D., 2004. A predictive model of edge effects. Ecology 85, 2917–2926. https://doi.org/10.1890/03-8021.

Shamyuktha, R., Amudha, J., Aiswariya Milan, K., 2022. A machine learning framework for classification of expert and non-experts radiologists using eye gaze data. In: 2022 IEEE 7th International Conference on Recent Advances and Innovations in Engineering (ICRAIE), Mangalore, India, pp. 314–320. https://doi.org/10.1109/ICRAIE56454.2022.10054277.

swisstopo, 2022a. Federal Office of Topography swisstopo. swissALTI3D. URL: https://www.swisstopo.admin.ch/en/geodata/height/alti3d.html.

swisstopo, 2022b. Federal Office of Topography swisstopo. swissSURFACE3D. URL: https://www.swisstopo.admin.ch/de/geodata/height/surface3d.html.

Valizadegan, H., Nguyen, Q., Hauskrecht, M., 2013. Learning classification models from multiple experts. J. Biomed. Inform. 46, 1125–1135. https://doi.org/10.1016/j.jbi.2013.08.007.

Verhelst, T.E., Vangansbeke, P., De Frenne, P., D'hont, B., Ponette, Q., Willems, L., Verbeeck, H., Calders, K., 2023. Forest edge structure from terrestrial laser scanning to explain bird biophony characteristics from acoustic indices. Remote Sensing in Ecology and Conservation doi:10.1002/rse2.334.

Wang, Z., Ginzler, C., Waser, L.T., 2020. Assessing structural changes at the forest edge using kernel density estimation. For. Ecol. Manage. 456, 117639. https://doi.org/10.1016/j.foreco.2019.117639.

Waser, L.T., Fischer, C., Wang, Z., Ginzler, C., 2015. Wall-to-wall forest mapping based on digital surface models from image-based point clouds and a nfi forest definition. Forests 6, 4510–4528. https://doi.org/10.3390/f6124386.

Waser, L.T., Rüetschi, M., Psomas, A., Small, D., Rehush, N., 2021. Mapping dominant leaf type based on combined Sentinel-1/-2 data–Challenges for mountainous countries. ISPRS J. Photogrammetry Remote Sensing 180, 209–226. https://doi.org/10.1016/j.isprsjprs.2021.08.017.

Webster, C., Essery, R., Mazzotti, G., Jonas, T., 2023. Using just a canopy height model to obtain lidar-level accuracy in 3d forest canopy shortwave transmissivity estimates. Agric. For. Meteorol. 338, 109429. https://doi.org/10.1016/j.agrformet.2023.109429.

Webster, C., Mazzotti, G., Essery, R., Jonas, T., 2020. Enhancing airborne lidar data for improved forest structure representation in shortwave transmission models. Remote Sens. Environ. 249, 112017. https://doi.org/10.1016/j.rse.2020.112017.

Wehrli, I., 2015. Erfassung der Struktur und ökologische Bewertung von Waldrändern mit LiDAR- und anderen räumlichen Daten. Entwicklung eines Schlüssels zur ökologischen Waldrandbewertung mit Geodaten für den Kanton Aargau. MSc Thesis. ETH Zurich, Zurich, Switzerland.

White, J.C., Coops, N.C., Wulder, M.A., Vastaranta, M., Hilker, T., Tompalski, P., 2016. Remote sensing technologies for enhancing forest inventories: A review. Canadian J. Remote Sensing 42, 619–641. https://doi.org/10.1080/07038992.2016.1207484.

White, J.C., Wulder, M.A., Varhola, A., Vastaranta, M., Coops, N.C., Cook, B.D., Pitt, D., Woods, M., 2013. A best practices guide for generating forest inventory attributes from airborne laser scanning data using an area-based approach. The Forestry Chronicle 89, 722–723.

Wuyts, K., De Schrijver, A., Vermeiren, F., Verheyen, K., 2009. Gradual forest edges can mitigate edge effects on throughfall deposition if their size and shape are well considered. For. Ecol. Manage. 257, 679–687. https://doi.org/10.1016/j.foreco.2008.09.045.